Journal of proteome research

Article

Cite This: J. Proteome Res. 2019, 18, 1078−1087

pubs.acs.org/jpr

Deuterium-Free, Three-Plexed Peptide Diethylation for Highly Accurate Quantitative Proteomics

Jaehun Jung,[§] Kyowon Jeong,[†,‡] Yeon Choi,[†,‡] Sun Ah Kim,[†,‡] Hyunjoon Kim,[†,‡] Joon Won Lee,[§] V. Narry Kim,[†,‡] Kwang Pyo Kim,[§] and Jong-Seo Kim*[,†,‡]

[†]Center for RNA Research, Institute for Basic Science (IBS), Seoul 08826, Korea

[‡]School of Biological Sciences, Seoul National University, Seoul 08826, Korea

[§]Department of Applied Chemistry, College of Applied Science, Kyung Hee University, Yongin 17104, Korea

Supporting Information

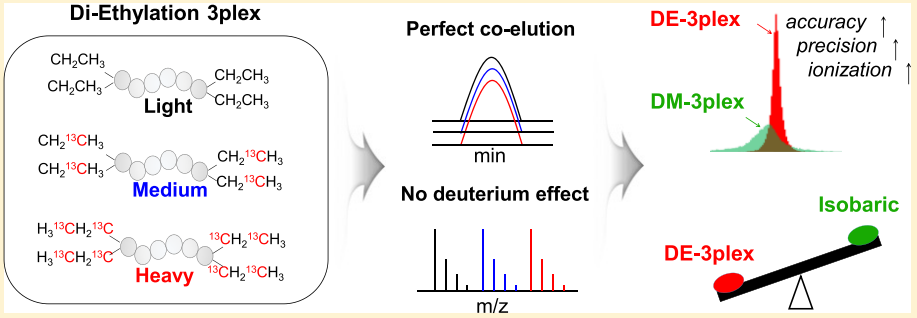

ABSTRACT: The deuterium, a frequently used stable isotope in isotopic labeling for quantitative proteomics, could deteriorate the accuracy and precision of proteome quantification owing to the retention time shift of deuterated peptides from the hydrogenated counterpart. We introduce a novel three-plexed peptide "diethylation" using only ^{13}C isotopologues of acetaldehyde and demonstrate that the accuracy and precision of our method in proteome quantification are significantly superior to the conventional deuterium-based dimethylation labeling in both a single-shot and multidimensional LC−MS/MS analysis of the HeLa proteome. Furthermore, in time-resolved profiling of *Xenopus laevis* early embryogenesis, our 3-plexed diethylation outperformed isobaric labeling approaches in terms of the quantification accuracy or the number of protein identifications, generating more than two times more differentially expressed proteins. Our cost-effective and highly accurate 3-plexed diethylation method could contribute to various types of quantitative proteomics applications in which three of multiplexity would be sufficient.

KEYWORDS: *diethylation, dimethylation, quantitative accuracy, deuterium effect, isotopic labeling, isobaric labeling*

INTRODUCTION

LC−MS-based quantitative proteomics is being magnified as an indispensable technique to discover the functional key proteins in dynamic cellular processes of various biological samples.[1,2] Unlike in the next-generation DNA/RNA sequencing, the label-free quantification approach in proteomics has been considered to be less accurate than labeling-based approaches due to its run-to-run variation as well as limited sequencing depth of LC−MS/MS.[3] Thus to achieve more accurate and reproducible proteome analyses, two orthogonal labeling strategies, that is, isobaric and isotopic labeling schemes, have been developed during the past decade.[4−11]

Isobaric labeling of peptides leads to an identical mass shift of precursor ions but yields distinguishable quantitative reporter ions via fragmentation in the gas phase such as MS/MS (MS2) so that conceptually all identifiable peptides could be quantifiable within the multiplexed analysis.[5,6] However, a major drawback of this method regarding quantification accuracy has been reported: Coeluting other peptide ions within the isolation mass window of the precursor ion can be cofragmented in collision cell, distorting reporter ion intensities and resulting in compressed fold changes.[12,13] Although this issue can be solved in part by introducing an additional collision mode of fragment ions (that is, MS3),[14,15] which is solely allowed for a couple of high-end instruments, the quantitatively interfering feature of isobaric labeling is often observed even in the MS3 approach.[16]

Conversely, the isotopic labeling via chemical or metabolic process differentiates the mass of precursor ions with stable isotopes at the MS1 level. Thus the interference effect of other precursor ions can be bypassed even with commonly used mass spectrometers such as Q-TOF or Q-Orbitrap, resulting in superior quantification accuracy to isobaric labeling.[17,18] Out of various isotopic labeling techniques, the 3-plexed dimethylation (DM) of peptides using formaldehyde isotopologues

Received: October 3, 2018
Published: January 14, 2019

DOI: 10.1021/acs.jproteome.8b00775
J. Proteome Res. 2019, 18, 1078−1087

containing deuterium has been predominantly adopted during the past decade for various biological and medical proteomics research,[8,19−26] mainly due to the low cost of reagents and the robust chemistry without side reaction.[19] In DM-3plex labeling, however, the different numbers of deuteriums between the labeling channels often incur a considerable discrepancy of retention times within a given labeled peptide. This is because the deuterated species are slightly more hydrophilic than the hydrogenated counterpart (known as the "deuterium effect").[27,28] This "deuterium effect" can largely compromise the quantification accuracy and result in underestimated fold changes.[29]

Here we report a novel 3-plexed diethylation (DE) method for highly accurate quantitative proteomics, in which DE is acetaldehyde-based reductive alkylation of peptides.[30−32] Because all mass shifts are introduced by ^{13}C isotopologues of acetaldehyde, our DE-3plex method is free from the deuterium effect; therefore, the multiplexed peptides are coeluted in LC−MS analysis. Also, ^{13}C isotopologues of acetaldehyde are all commercially available and cost-effective overall (<$10 for labeling of 100 μg proteome). Our systematic comparison via both single-shot and multidimensional analyses demonstrates that the DE-3plex labeling significantly outperforms the conventional DM-3plex labeling in terms of both quantitative accuracy and precision. For instance, the proteins with the 10-fold change were accurately quantified in the DE-3plex, whereas they were not accurately quantified in the DM-3plex.

Besides, when compared with isobaric labeling (tandem mass tag (TMT)),[6] the DE-3plex method shows superior quantification accuracy or a greater number of identified proteins with comparable accuracy, depending on the instrumental mode in isobaric labeling, from the analysis of the maternal to zygotic transition (MZT) of *Xenopus laevis* embryos (stages 1, 8, and 13). We believe that with all of these advantages the new DE-3plex labeling could be the method of choice for 3-plexed proteomics applications.

EXPERIMENTAL SECTION

Enolase and HeLa Sample Preparation

Enolase from baker's yeast was purchased from Sigma-Aldrich. HeLa cells were grown in DMEM supplemented with 10% fetal bovine serum. Cell pellets were lysed in 8 M urea with 50 mM ammonium bicarbonate (ABC, pH 8.5) containing 1× Halt protease inhibitor (Thermo Fisher). The HeLa lysates and yeast enolase samples were reduced by 10 mM DTT for 1 h at 37 °C, followed by alkylation with 40 mM iodoacetamide for 30 min at 37 °C in the dark. Samples were diluted with 50 mM ABC to <1 M of urea concentration, followed by LysC (Wako) digestion with 2% (w/w) at 37 °C for overnight. The remaining activity of LysC was quenched by acidifying the sample with 0.4% TFA, and the resulting digests were desalted by C18 SPE cartridge (Supelco).

Xenopus laevis Embryo Sample Preparation

X. laevis were obtained from NASCO and the Korean *Xenopus* Resource Center for Research. Embryos were collected as described.[33] In brief, 800 units of human chorionic gonadotrophin (Dae Sung Microbiological Laboratories) was injected into a female *X. laevis* 12 h before collection. Eggs were obtained in 1× MMR (Marc's Modified Ringer) and in vitro fertilized using macerated testis. Fertilized embryos were dejellied with 2% cysteine, pH 7.8. Nieuwkoop and Faber stages were used for developmental staging.

A single embryo of *Xenopus laevis* in each stage (1, 8, 13) was individually lysed with lysis buffer (250 mM sucrose, 1% NP-40 substitute (Sigma), 5 mM EDTA, 1× Halt protease inhibitor, and 20 mM HEPES (pH 7.2)), followed by deyolking.[34] 40 μg of deyolked proteome from a single embryo was further denatured at 90 °C for 10 min, and cysteine residues were alkylated. The alkylated sample was subjected to in-filter LysC digestion using a 30 kDa MWCO Amicon filter (0.5 mL, Millipore), followed by quenching of protease and desalting, as described above. The resulting 20 μg of LysC digest for each stage was preserved for the next labeling experiments.

Diethylation of Peptides and Other Chemical Labeling

The lyophilized peptides were resuspended with 100 mM sodium acetate buffer (pH 5.5) for reductive alkylation.[35] First, for DE, one of three acetaldehyde ^{13}C isotopologues (CH_3CHO (Sigma), $CH_3{}^{13}CHO$ (Sigma), and $^{13}CH_3{}^{13}CHO$ (Cambridge Isotope Laboratories) for light, medium, and heavy labeling, respectively) was added to the peptides sample to be of 500 mM concentration, followed by the addition of $NaBH_3CN$ (Sigma) to be 250 mM (Figure 1a). For DM, a formaldehyde isotopologue (CH_2O (Sigma), CD_2O (CDN Isotopes), and $^{13}CD_2O$ (Sigma) for light, medium, and heavy labeling, respectively) was combined with the adequate reducing reagent ($NaBH_3CN$ for light and medium labeling or $NaBD_3CN$ (CDN Isotopes) for heavy labeling) (Figure S1a). All dimethylating reagents were added at same concentration, as in the case of DE. Samples were briefly vortexed and incubated for 1 h at room temperature (RT) in the Thermomixer (Eppendorf) with 500 rpm. The reductive alkylation process can be repeated once more if necessary. The reductive alkylating reagents were quenched by the addition of 1 M ABC solution to be 500 mM. TMT labeling of *X. laevis* samples was carried out by following the manufacturer's recommendation. Twenty μg of digests from a single embryo for each stage was divided into two identical aliquots and subjected to duplicate TMT labeling, as follows: TMT-126 and -129 for stage 1, TMT-127 and -130 for stage 8, TMT-128 and -131 for stage 13.

Multidimensional Mid-pH RPLC Fractionation

Microscale (20 μg (HeLa) or 30 μg (*X. laevis*)) mid-pH reversed-phase liquid chromatography (RPLC) off-line fractionation was carried out using an in-house packed 200 μm i.d. C18 capillary column operated by nanoACQUITY ultra-performance liquid chromatography (UPLC) (Waters) at 3 μL/min of flow rate with a linear gradient of solvent A (10 mM ABC in water) and solvent B (10 mM ABC in 90% ACN) from 2 to 40% of solvent B for 90 min. The eluent was automatically collected into the 96-well plate per each minute using Triversa NanoMate (Advion) and then concatenated to 6 (HeLa) or 24 (*X. laevis*) fractions.

LC−MS/MS or LC−MS3 Analysis

LC−MS/MS analysis of enolase and HeLa samples for the comparison of DE- and DM-3plex was carried by Q-Exactive Orbitrap MS (Thermo Fisher Scientific) coupled to a nanoACQUITY UPLC equipped with an in-house-packed trap (150 μm i.d. × 3 cm) and analytical column (75 μm i.d. × 100 cm) using 3 μm of Jupiter C18 particle (Phenomenex). A linear gradient of solvent A (water with 0.1% formic acid) and

DOI: 10.1021/acs.jproteome.8b00775
J. Proteome Res. 2019, 18, 1078−1087

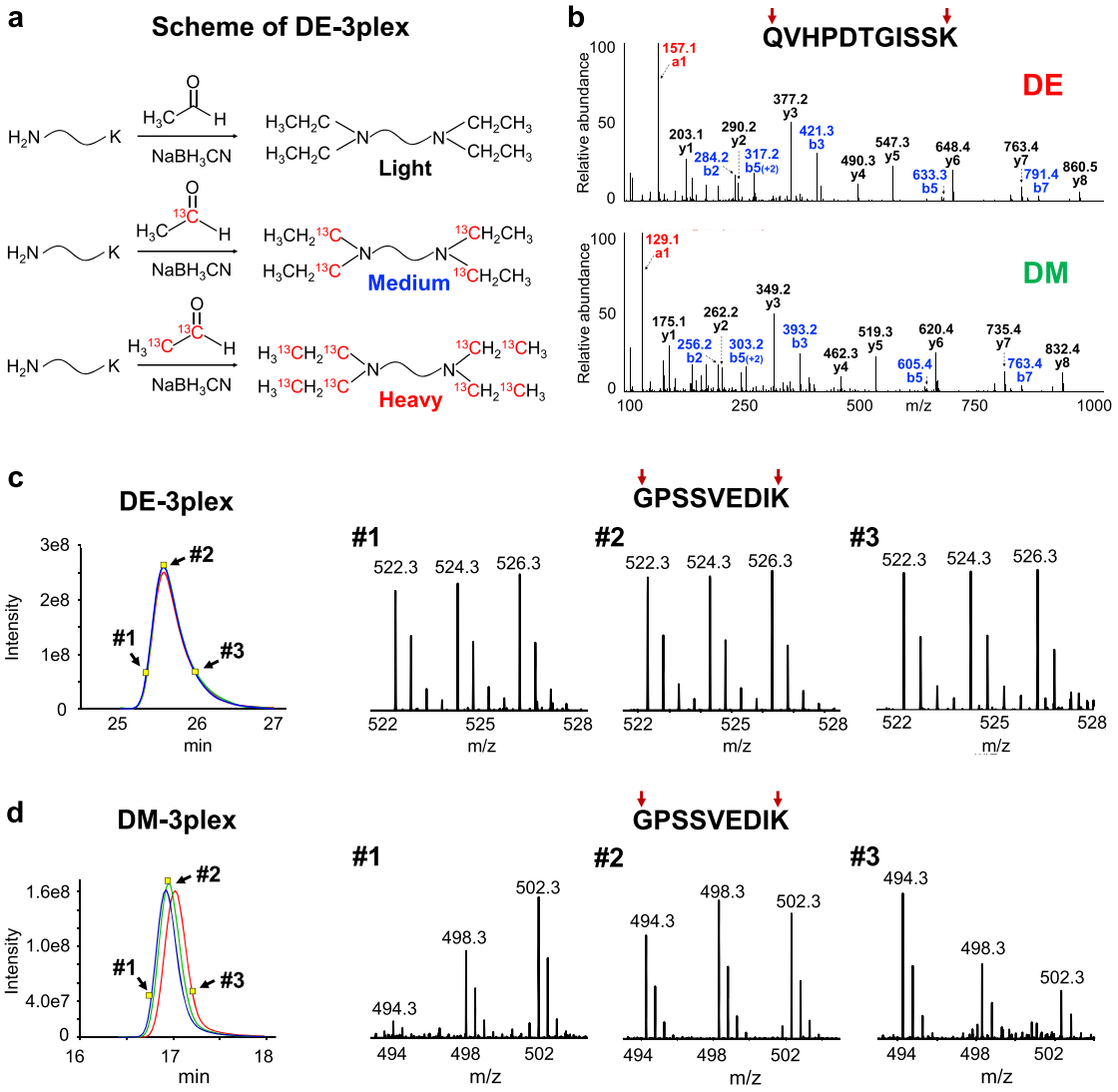

Figure 1. Three-plexed peptide diethylation (DE). (a) Scheme for 3-plexed DE of Lys-C digested peptides using acetaldehyde ^{13}C isotopologues. (b) Representative MS/MS spectra of DE-labeled (top) and dimethylation (DM)-labeled peptide (bottom) for QVHPDTGISSK. Superimposed extracted ion chromatograms (XICs; light, red line; medium, green line; heavy, blue line) and full mass spectra of DE-3plexed (c) and DM-3plexed GPSSVEDIK (d) at several elution time points (#1, #2, and #3) spanning from the beginning to the end of the XIC. Red arrows indicate the labeled amino groups.

solvent B (ACN with 0.1% formic acid) in ACN) was applied at a flow rate 300 nL/min: 5 to 10% solvent B for the initial 5 min and 10 to 40% solvent B for the next 90 min.

X. laevis embryogenesis was profiled using Orbitrap Fusion Lumos Tribrid MS (Thermo Fisher Scientific) coupled to the aforementioned LC system. For the MS2-only method for the analyses of DE-3plex and TMT-MS2 samples, full MS scans (m/z 300−1500) were acquired at a resolution of 60k (at m/z 200). Higher-energy collisional dissociation (HCD) fragmentation was performed under 30% of normalized collision energy (NCE) via precursor isolation within 1.6 Th of window. The MS2 scans were acquired at a resolution of 15k (ITmax 30 ms and AGC 2E4). For the MS3 analysis, the most intense 10 ions were first isolated at 0.5 Th of precursor isolation width under the identical full MS scan settings for CID MS2 in ion trap (ITmax 150 ms and AGC 4E3). The 10 most intense MS2 fragment ions were synchronously isolated for HCD MS3 (AGC 1.5E5, ITmax 250 ms, and NCE 55%) at 2 m/z of isolation width. All of the raw mass data sets have been deposited to the PRIDE Archive (ProteomeXchange) with the data set identifier PXD012117.

Database Searching and Quantitative Analysis

The MaxQuant suite[36] (ver. 1.5.2.8) was used for the quantitative analysis of all of the diethylated and dimethylated samples. The UniProt human database (March 2016) or PHROG reference set[37] was used, and the false discovery rate (FDR) of the protein group and peptide spectrum match (PSM) were set to <1%. For 3-plexed modifications on the N-terminus and lysine, 28.0313, 32.0564, and 36.0756 Da were filled in as the light, medium, and heavy labels, respectively, for DM, whereas 56.0626, 58.0693, and 60.0670 Da were used for DE. More than two nonredundant peptides for a specific protein group were used for protein quantification.

Proteome Discoverer (PD) ver. 2.1 (Thermo Fisher Scientific), which is the most popular software platform for TMT labeling, was used for the quantitative analysis of TMT-labeled *X. laevis* data sets. The assignment of MS2 spectra was carried out using the SEQUEST algorithm, and the resulting

DOI: 10.1021/acs.jproteome.8b00775
J. Proteome Res. 2019, 18, 1078−1087

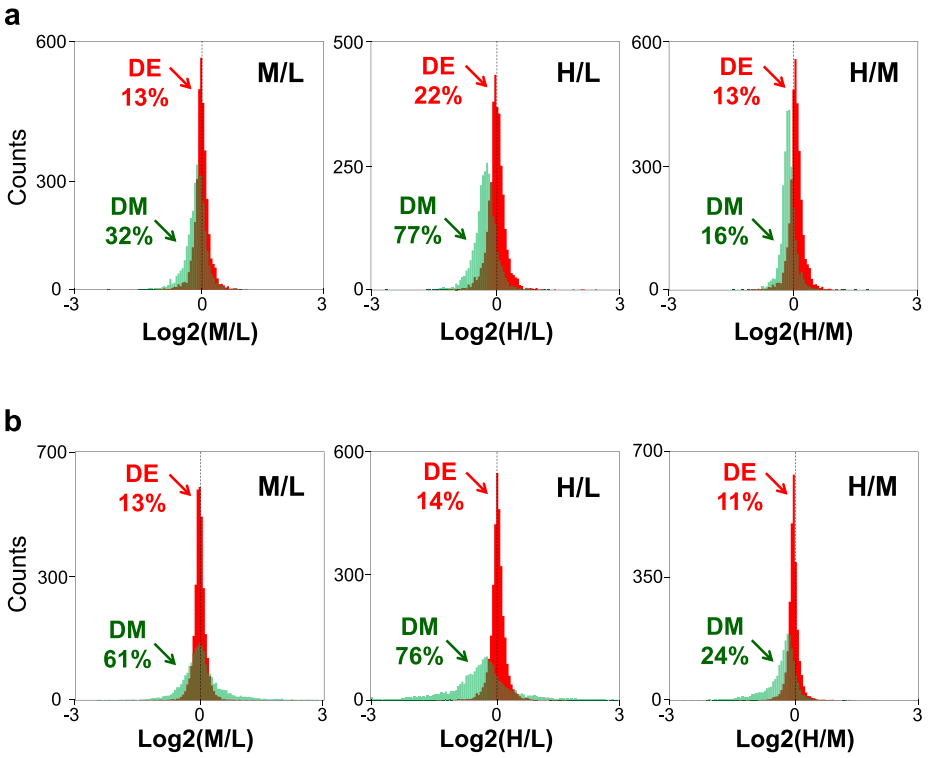

Figure 2. Quantitative accuracy and precision of DE-3plex versus DM-3plex in HeLa. Superimposed histograms of peptide ratios (medium to light (M/L), heavy to light (H/L), and heavy to medium (H/M)) from DE-3plex (red) and DM-3plex (green) methods, respectively, in an equimolar mixture of labeled HeLa cell lysate (a) in a single-shot LC−MS/MS analysis and (b) in multidimensional LC−MS/MS analyses. Inserted % numbers mean % CV value for the analysis.

peptide hits were filtered at maximum 1% FDR by the Percolator algorithm. Carbamidomethylation of cysteine and TMT labeling of lysine and peptide N-terminus were set as fixed modifications, whereas the methionine oxidation was considered as a variable modification. Full Lys-C specificity with up to two missed cleavage sites was applied. Mass tolerances for precursor and fragment ions were set to 10 ppm and 0.6 Da, respectively. The reporter ion ratios reported from PD were adjusted by applying the isotopic correction factors of the TMT kit provided by the manufacturer. Only all reporter ions containing spectra were designated as "quantifiable spectra".

For the clustering analysis, $\log_2$ fold changes between embryonic stages were calculated. The *k*-means clustering of $\log_2$ fold changes was done using the SciPy package, open-source scientific tools for Python (http://www.scipy.org). Data analysis and visualization following clustering analysis were carried out by in-house software.

Assessing Quantification Precision of DE-3plex-, TMT-MS2-, and TMT-MS3-Labeled *X. laevis* Samples

The precision analysis was assessed by gathering the peptides matching to a single protein and measuring the CV values of their quantity ratios (as such peptides are expected to have the same ratio). In detail, per protein with more than three matching peptides, we examined the CV values of the peptide quantity ratios between stages 1 and 8, 8 and 13, and 1 and 13. By drawing the histograms for CV values obtained from the proteins, the precision was assessed. For a fair comparison, we used only overlapping peptide−protein matches found in two comparison sets. For this analysis, we used only the first sample of the two replicates. Only nonredundant peptides were counted, and the proteins that do not make a protein group were selected. Per protein, the ratio CV values were calculated for both labeling schemes and used to draw Figure 4c,d.

RESULTS AND DISCUSSION

Three-Plexed Peptide Diethylation (DE-3plex) Using ^{13}C Isotope

Although the conventional DM-3plex has been used in numerous quantitative proteomics studies, the quantification accuracy of the method has been often doubtful due to the innate "deuterium effect" originated from the use of deuterated formaldehydes and cyanoborodeuteride[8,19] (Figure S1a). To solve this chronic issue, our DE-3plex method uses only the ^{13}C isotope to introduce mass shifts. Figure 1a shows that at least 4 Da of mass spacing (2 Da at N-terminus and 2 Da at lysine residue) between labeling channels can be obtained via reductive dialkylation of LysC-digested peptides using ^{13}C forms of acetaldehyde (acetaldehyde-1-^{13}C and acetaldehyde-$^{13}C_2$). The DE of peptides shows quantitative labeling efficiency on primary amines in HeLa (Table S1). Also, the fragmentation pattern of diethylated peptides was very similar to that of dimethylated ones, yielding a characteristic a1 ion[38,39] (Figure 1b and Figure S1b), probably due to very close gas-phase basicity between dialkyl amines.[40]

As expected, the superimposed extracted ion chromatograms (XICs) of individual labeling channels (light, medium, and heavy) in DE-3plex showed a complete coelution pattern (Figure 1c), whereas the counterpart from DM-3plexed peptide showed a sequential elution pattern (Figure 1d), which is known as the deuterium effect.[27,28] Consequently, the diethylated peptides showed consistent relative ratios between

DOI: 10.1021/acs.jproteome.8b00775
J. Proteome Res. 2019, 18, 1078−1087

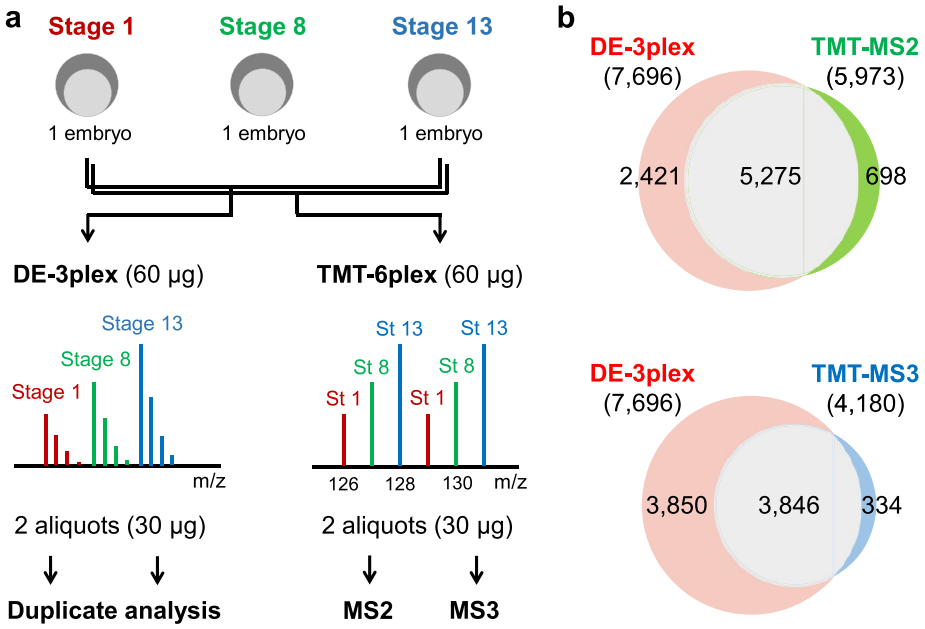

Figure 3. Temporal proteomics design and identification results in early embryogenesis of *Xenopus laevis*. (a) Experimental design for the comparative evaluation of the DE-3plex method with isobaric TMT-labeling approaches. (b) Comparison of identified protein groups between DE-3plex and TMT-MS2 (top) and between DE-3plex and TMT-MS3 (bottom), respectively. The numbers of proteins groups were from a single replicate data set only for the individual method.

channels at all elution time points spanning from the beginning to the end of the XICs (Figure 1c). However, the dimethylated peptides showed significantly fluctuating intensity ratios. In particular, the elution time shift between heavy (blue line) and light channels (red line) was substantial, resulting in the most distorted intensity ratios in the DM-3plex method (Figure 1d).

Enhanced Ionization and Profiling Depth from Peptide Diethylation

In the LC−MS/MS data set from an equimolar mixture composed of nonlabeled (NL), dimethylated, and diethylated HeLa peptides, we found that the average intensity ratios of diethylated and dimethylated over NL peptides were 4.0 and 1.8, respectively (Figure S2a, Table S2). This result indicates that the electrospray ionization efficiency of diethylated peptides is higher than those of the dimethylated peptides as well as the original NL peptides. The enhanced ionization might be attributed to more favorable desolvation of diethylated peptides because the diethylated peptides are eluted at later retention time with higher organic solvent composition than NL or even dimethylated peptides (Figure S2b). The enhanced ionization from DE over DM was confirmed in the large-scale data set as well. The area of total ion chromatogram (TIC) from diethylated sample was about two times higher than that from the dimethylated sample under the identical LC−MS/MS setting (Figure S2c, Table S3).

The enhanced ionization of diethylated peptides positively affected the proteome profiling depth. When the diethylated LysC digest of HeLa lysate (20 μg) was subject to LC−MS/MS analysis via mid-pH RPLC fractionation, 23 and 12% more of nonredundant peptides and protein groups, respectively, than dimethylated sample were identified at 1% FDR on the same analysis setting and scale (Figure S2d,e and Table S4). Considering that both labeling schemes show a very similar fragmentation pattern (Figure 1b and Figure S1b), the improved profiling depth from DE over the DM method can be credited to the enhanced ionization efficiency of diethylated peptides.

Notably, in the very early elution time range, a number of nonredundant peptides were exclusively identified in the DE over the DM sample (Figure S2f and Table S5). The histograms of exclusively identified peptides from DE and DM samples, respectively, along with the predicted normalized elution times (pNETs)[41] showed that a much larger number of hydrophilic peptides with <0.15 of pNET were identified in the DE sample. This observation indicates that those exclusively identified hydrophilic peptides in the DE sample are safely recovered and well-separated with enhanced sensitivity by virtue of DE labeling; otherwise, they are likely to be lost during the sample cleanup or loading step. Intriguingly, the boosting capability of DE in hydrophobicity also suggests that DE-3plex could be used for the multiplexed RPLC−MS analysis of amine-containing metabolites,[42] which otherwise are hardly retained on the C18 stationary phase.

Highly Accurate Proteome Quantification by DE-3plex Method

The proteome quantification accuracy and precision of the DE-3plex method were comparatively assessed with the DM-3plex method in both single-shot and multidimensional LC−MS/MS analyses (Figure S3).

In a Single-Shot Analysis. The equimolar mixtures of all three light (L), medium (M), and heavy (H) labeling channels were prepared for both DE and DM using the individually labeled LysC digest of yeast enolase or HeLa cell lysate. The samples were subsequently subject to a single-shot LC−MS/MS analysis in triplicate. First, the DE-3plex labeling of enolase peptides yielded peptide quantification ratios quite close to the expected ratio of 1.00 (e.g., 1.03 (M/L), 1.04 (H/L), and 1.01 (H/M) on average from triplicate analysis), whereas the dimethylated peptides showed rather inaccurate fold changes of 0.66 (M/L), 0.73 (H/L), and 1.13 (H/M) (see Figure S4 and Table S6). Furthermore, the variation of fold change in the

DOI: 10.1021/acs.jproteome.8b00775
J. Proteome Res. 2019, 18, 1078−1087

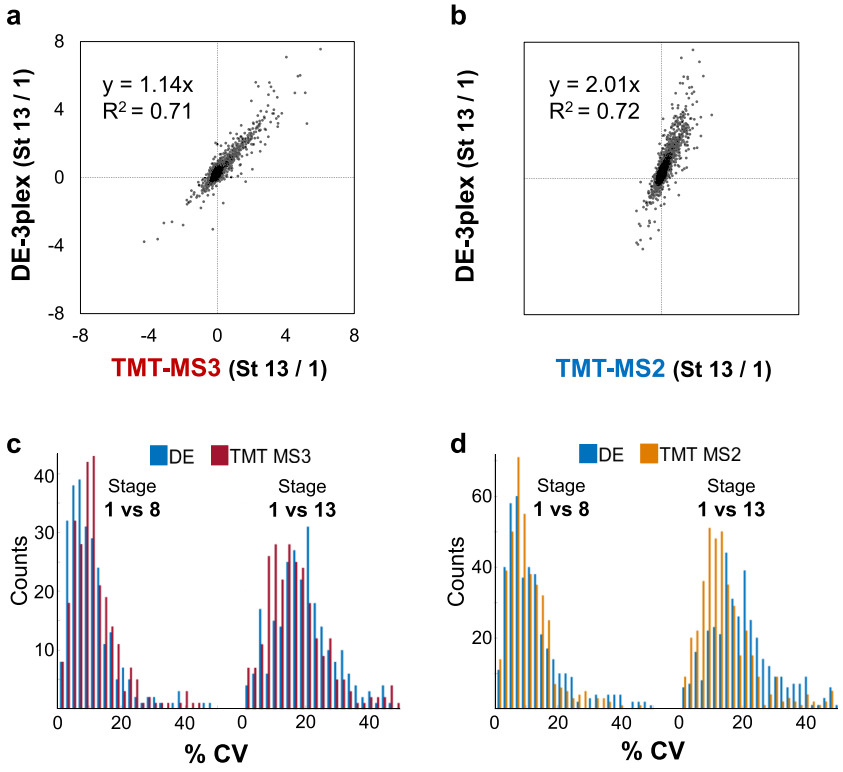

Figure 4. Quantitative accuracy and precision of DE-3plex compared with isobaric labeling in embryogenesis of *X. laevis*. Scatter plots of protein quantification ratio on the log2 scale (stage 13 to 1) from DE-3plex versus TMT-MS3 (a) and versus TMT-MS2 (b), respectively. Histographic % CV distribution of peptide quantity ratios with the same matching protein for DE and TMT-MS3 (c) and for DE and TMT-MS2 (d). Because peptides with the same matching protein are expected to have the same quantity ratios, their CV values are used to measure the quantification precision. (See the Experimental Section for details.)

DE-3plex method was much smaller than that in DM-3plex, highlighting the outperforming precision of the DE-3plex method (Figure S4). These results collectively show that the coelution character of DE-3plex favorably affects the quantification accuracy and precision. The superimposed histograms in Figure 2a demonstrate that DE-3plex is a more accurate and precise method than DM-3plex, even in the highly complex sample such as HeLa lysate: The median ratios of peptides were 1.02 (M/L), 1.00 (H/L), and 1.02 (H/M) with 13∼20% coefficient of variation in the equimolarly 3-plexed DE sample, whereas they were 0.95 (M/L), 0.83 (H/L), and 0.90 (H/M) with higher CV (16∼77%) than DE in the equimolar mixture of DM-labeled samples (Table S7).

We also benchmarked DE-3plex in various mixtures with known ratios (L/M/H 1:2:4 and 1:5:10) as compared with DM-3plex in a single-shot analysis. Lau et al.[29] reported that protein ratio compression was observed even at 5:1 H/L ratio in DM-3plex, and it became worse at higher H/L ratio such as 10:1. We also observed consistent ratio compression at 4:1 H/L ratio in the DM-3plex method, 3.3 H/L ratio for the 4:1 mixture, and 7.9 H/L ratio for the 10:1 mixture (Figure S5, Table S8). The measured quantification ratio from the DE-3plex method, on the contrary, was almost exactly proportional to the expected ratio (Figure S5), demonstrating its highly accurate response in such a high dynamic range.

In Multidimensional Analysis. The 20 μg of equimolar mixtures for DE-3plex and DM-3plex, respectively, were subject to multidimensional LC−MS/MS analysis using mid-pH microscale RPLC offline fractionation.[43] In brief, each equimolar mixture sample was separated on a capillary C18 column (i.d. 200 μm) at pH 8 and fractionated into 96 wells. Then, the 96 wells were concatenated into six fractions,[44] which were subject to the final LC−MS/MS analysis.

Figure 2b illustrates the histographic distribution of the quantification ratio of peptides between labeling channels. The results from both DE-3plex (1.02 (M/L), 1.03 (H/L), and 1.01 (H/M)) and DM-3plex (0.98 (M/L), 0.83 (H/L), and 0.85 (H/M)) were fairly close to the expected ratio (1.00). However, the quantification precision in DM-3plex coupled to multidimensional analysis[45,46] was significantly inferior (24∼76% CV) to that of DE-3plex (11∼14% CV). This shows that the fold-change result of an individual protein from the multidimensional analysis of DM-3plex method would not be as reliable as that of DE-3plex (Tables S9 and S10). Collectively, like the case of a single-shot analysis, these results clearly demonstrate that DE-3plex generates highly accurate and precise quantification results in the large-scale proteomics experiment via multidimensional separation.

Proteomic Profiling of *X. laevis* Embryogenesis Using DE-3plex versus Isobaric Labeling

We applied the DE-3plex method to *X. laevis* embryos (stages 1, 8, and 13) to explore the landscape of proteome change in *X. laevis* early embryogenesis. Also, the isobaric labeling was carried out in parallel for the comparison with DE-3plex. Via deyolking, 20 μg of LysC digest from a single embryo in each stage was individually labeled by DE-3plex method, that is, stage 1 by DE-light, stage 8 by DE-medium, and stage 13 by DE-heavy channel (Figure 3a, left). Pooled sample (60 μg) of all three stages was divided into two aliquots; then, each aliquot was subject to duplicate multidimensional LC−MS/

DOI: 10.1021/acs.jproteome.8b00775
J. Proteome Res. 2019, 18, 1078−1087

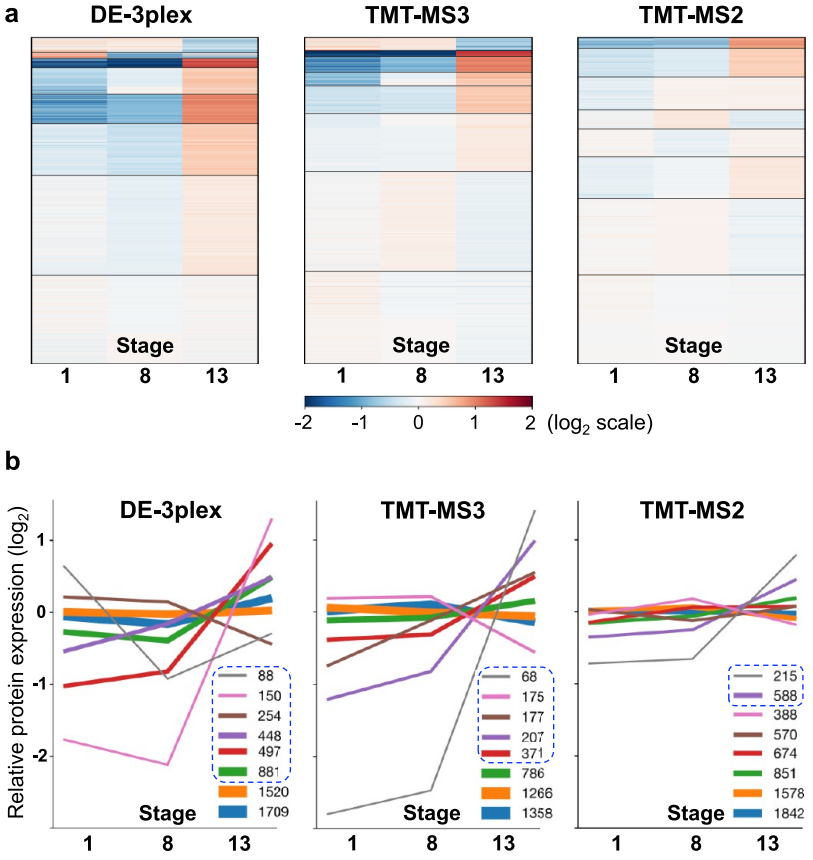

Figure 5. Heat map (a) and clustering analysis (b) of temporal protein expression level in embryogenesis of *X. laevis* from DE-3plex, TMT-MS3, and TMT-MS2 methods, respectively. *k*-means clustering of $\log_2$ protein fold changes into eight clusters was carried out. The thickness of the median line and inserted number indicate the protein number in the cluster. The blue dotted box represents the DEP clusters exceeding the median temporal change threshold (1.5-fold).

MS analysis via mid-pH microscale RPLC offline fractionation. In the case of TMT labeling, we allowed the use of the higher multiplexity for the duplicate analysis of the three stages (total 6plex): 20 μg of deyolked digest sample from a single embryo was divided into two identical aliquots and subjected to duplicate TMT labeling. One fractionated set of the pooled TMT-6plex sample was analyzed by MS2 mode only (TMT-MS2), whereas the other set was analyzed by MS3 mode[14,15] (TMT-MS3) (Figure 3a, right).

From the limited sample amount (30 μg of peptides equivalent to 1.5 embryos), we successfully identified nearly 8k protein groups (7696) in a single replicate of DE-3plexed sample from PD analysis at 1% of protein level FDR (Figure 3b). Intriguingly, the DE-3plex labeling generated a larger number of protein groups than TMT-MS2 or TMT-MS3 under the identical analysis platform (Figure 3b, Figure S6a, and Table S11). Given that the TIC area sum of all fraction data sets was comparable between DE-3plex and TMT-MS2 data sets (Figure S6a), the larger number of protein identification from the DE-3plex data set indicates that the solid character of the C−N σ bond in DE for gas-phase fragmentation might be more beneficial to protein identification than the innate fragile feature of the TMT moiety yielding complex fragment ions such as complementary ion clusters,[47] despite the lower peptide sampling efficiency in DE-3plex owing to increased precursor ion complexity.

The quantitative fold changes of the DE-3plex method between stages showed highly positive correlation with isobaric labeling (Figure 4a,b) and comparable quantitative precision to the isobaric method (Figure 4c,d). We found that the quantitative dynamic range of DE-3plex was quite similar to that of TMT-MS3 (Figure 4a) but far wider than that of TMT-MS2 (Figure 4b). These results indicate that the proteome quantification by the DE-3plex method is as accurate as that by the TMT-MS3 approach, which is known to have significantly higher quantification accuracy[14,15] but longer sequencing duty cycle (and thus reduced identification[48]) than the TMT-MS2 approach. When considering that the TMT-MS3 mode is available on only a couple of high-end instrument types such as the Fusion Tribrid system, the quantitative capability of DE-3plex by common mass spectrometers, that is, TMT-MS3-comparable quantification accuracy with more comprehensive identification, can be particularly beneficial for researchers using normal instruments. The highly accurate quantification power of DE-3plex was confirmed again in the comparison with another isobaric labeling (iTRAQ)[49] carried out in identical stages of frog embryos (Figure S7a). To crosscheck our result, we referred to the previously reported Western blot (WB) assay of a few selected proteins, Xcdc6[49] (Figure S7b) and Lin28A[48] (Figure S7c), and found that the DE-3plex results were well-matched with the WB data.

Notably, the heat map and clustering analysis of temporal expression level shows that DE-3plex generates a higher portion of protein groups classified as differentially expressed protein (DEP) clusters than isobaric labeling (Figure 5a, Figure S8, and Table S12). When applying a median temporal

DOI: 10.1021/acs.jproteome.8b00775
J. Proteome Res. 2019, 18, 1078−1087

change threshold (1.5-fold) for the DEP cluster, six DEP clusters with 2476 proteins including two clusters showing a maternally deposited and zygotically degraded pattern were observed in the DE-3plex, whereas four DEP clusters with a significantly reduced number of proteins (839 proteins) remained in TMT-MS3 (Figure 5b). Even worse, TMT-MS2 analysis resulted in ambiguous patterns of temporal change except only two compressed DEP clusters (Figure 5b). Regarding the use of protease, the trypsin digestion instead of Lys-C would be more optimal for TMT labeling because a greater number of proteins (≥30%) could be identified in tryptic digests compared with Lys-C digests, generating a higher number of DEPs for TMT-labeling approaches than this study. However, even if reflecting the potential gain from trypsin digestion, the possible DEP number in the TMT-MS2 or MS3 approach might not exceed that of DE-3plex in this biological context. Collectively, all of these observations support the fact that the DE-3plex method can be a general choice for the specific 3-plexed quantitative proteomics studies, representing a greater number of DEPs.

An innate drawback in our method would be the incompatibility to other proteases such as trypsin and Glu-C. To enable the three of multiplexity with ≥4 Da of mass spacing between channels, greater than or equal to two amino groups per peptide would be necessary, which could be obtainable from the use of Lys-C protease. With other proteases, the mass spacing between channels would be relatively small (2 Da), resulting in overlapping isotopic distributions and compromising the quantification performance. Thereby, our method could offer only duplex (light and heavy) for the research projects requiring other proteases or incompatible to Lys-C digestion.

Furthermore, the three of multiplexing power in our method might not be sufficient for most of the large-scale proteomics experiments where a large number of samples should be analyzed (e.g., medical proteomics experiments for biomarker discovery). However, we believe that the 3-plexed proteomics design including triple SILAC is still being actively used, and our method can contribute to that kind of experiments. For instance, in many biological experiments, comparative experiments between three conditions such as two experimental conditions with a wild-type control are common (e.g., starvation, inhibitor-treated, and normal media condition for ribophagy study).[50] In this type of biological study, the quantification accuracy should be reliable for biological discovery when dealing with subtly changed protein targets. As we demonstrated, because the DE-3plex method allows for highly accurate and precise quantification, this method can be valuably used for those quantitative proteomic studies in which three of multiplexity would be sufficient.

In conclusion, our newly developed 3-plexed peptide DE considerably improves the quantification accuracy and precision of the proteome compared with the conventional DM-3plex approach and thereby could be directly applied to other DM-based proteomics techniques or applications, for example, Terminomics (N- or C-TAILS)[20,21] or amino metabolome profiling.[51] Furthermore, our new method provides comparable quantification performance with a higher number of protein identifications to the MS3-based isobaric labeling method, which is allowed only by high-end instruments. We believe that our cost-effective and highly accurate DE-3plex method can contribute widely to much proteomics research including dramatically changing developmental systems such as early embryogenesis.

■ ASSOCIATED CONTENT

Supporting Information

The Supporting Information is available free of charge on the ACS Publications website at DOI: 10.1021/acs.jproteome.8b00775.

Figure S1. Scheme for 3-plexed DM of Lys-C digest using formaldehyde isotopologues. Representative MS/MS spectra of DE-labeled and DM-labeled peptide for DSYVGDEAQSK. Figure S2. Enhanced electrospray ionization from peptide diethylation. Figure S3. Experimental workflow for the comparison of DE-3plex with DM-3plex. Figure S4. Fold-change comparison of DE- and DM-3plexed enolase peptides. Figure S5. Comparison of quantitative dynamic range and accuracy between DE-3plex and DM-3plex. Statistical table for comparison of quantitative precision between two labeling methods. Figure S6. Comparison table showing the identified and quantifiable protein numbers from two independent analysis platforms in early embryogenesis of *Xenopus laevis*. Comparison of quantifiable protein groups between DE-3plex and TMT-MS2 and between DE-3plex and TMT-MS3, respectively. Figure S7. Scatter plot of protein quantification ratio on log2 scale (stages 13 to 1) from DE-3plex versus iTRAQ labeling. Fold-change plots of a few proteins, Xcdc6 and Lin28A, for which WB data are available in previous reports. Figure S8. Eight clusters classified by *k*-means clustering of log2 fold changes between each embryonic stages in DE-3plex, TMT-MS3, and TMT-MS2 data, respectively (PDF)

Table S1. Labeling efficiencies of diethylation and dimethylation in HeLa LysC digest at PSM level (XLSX)

Table S2. Enhanced ESI efficiency by peptide diethylation (XLSX)

Table S3. Enhanced ESI efficiency by peptide diethylation (XLSX)

Table S4. Identified protein group and unique peptide list from 24 fractions of DM-light and DE-light labeled HeLa LysC digest at 1% protein FDR using MaxQuant (XLSX)

Table S5. Exclusively identified peptide list with pNET between the same DM- and DE-labeled samples (XLSX)

Table S6. Quantitative accuracy and precision in a single-shot triplicate analysis in equimolarly DE- and DM-3plexed yeast enolase peptides, respectively (XLSX)

Table S7. Quantitative accuracy and precision in a single-shot triplicate analysis in equimolarly DE- and DM-3plexed HeLa LysC digest, respectively (XLSX)

Table S8. Quantitative accuracy and precision in premixed samples at known ratios (L/M/H 1:1:1, 1:2:4, and 1:5:10) using DE- and DM-3plexed HeLa LysC digest, respectively, at protein level and peptide level (XLSX)

Table S9. Quantitative accuracy and precision in multidimensional triplicate analysis at protein level (XLSX)

DOI: 10.1021/acs.jproteome.8b00775
J. Proteome Res. 2019, 18, 1078−1087

Table S10. Quantitative accuracy and precision in multidimensional triplicate analysis at peptide level (XLSX)

Table S11. Protein identification and temporal quantification results in early embryogenesis of *X. laevis* by MaxQuant and Proteome Discoverer in DE-3plex, TMT-MS2, and TMT-MS3 data (XLSX)

Table S12. Clustering analysis of temporal proteomics results in early embryogenesis of *X. laevis* *k*-means clustering of log2 fold changes between each embryonic stage was carried out in DE-3plex, TMT-MS2, and TMT-MS3 (XLSX)

AUTHOR INFORMATION

Corresponding Author

*Tel: 82-2-880-4434. Fax: 82-2-887-0244. E-mail: jongseokim@snu.ac.kr.

ORCID

Jong-Seo Kim: 0000-0002-8909-8440

Author Contributions

J.-S.K. and J.J. conceived the project. J.-S.K. developed the DE-3plex labeling. J.J. performed all of the experiments and analyzed the data. K.J. and Y.C. contributed to the analysis of *X. laevis* data. S.A.K. initially optimized reductive diethylation. H.K. provided *X. laevis* samples. J.W.L. contributed to microscale fractionation. V.N.K and K.P.K provided resources. J.J., K.J., and J.-S.K. wrote the manuscript with help of all other authors.

Notes

The authors declare no competing financial interest.

All of the raw mass data sets have been deposited to the PRIDE Archive (ProteomeXchange) with the data set identifier PXD012117.

ACKNOWLEDGMENTS

This work was supported by the fund from Institute for Basic Science of Korea (IBS-R008-D1).

REFERENCES

(1) Cravatt, B. F.; Simon, G. M.; Yates, J. R., 3rd The biological impact of mass-spectrometry-based proteomics. *Nature* **2007**, *450* (7172), 991−1000.

(2) Mallick, P.; Kuster, B. Proteomics: a pragmatic perspective. *Nat. Biotechnol.* **2010**, *28* (7), 695−709.

(3) Deracinois, B.; Flahaut, C.; Duban-Deweer, S.; Karamanos, Y. Comparative and Quantitative Global Proteomics Approaches: An Overview. *Proteomes* **2013**, *1* (3), 180−218.

(4) Lee, Y. H.; Han, H.; Chang, S. B.; Lee, S. W. Isotope-coded N-terminal sulfonation of peptides allows quantitative proteomic analysis with increased de novo peptide sequencing capability. *Rapid Commun. Mass Spectrom.* **2004**, *18* (24), 3019−3027.

(5) Choe, L.; D'Ascenzo, M.; Relkin, N. R.; Pappin, D.; Ross, P.; Williamson, B.; Guertin, S.; Pribil, P.; Lee, K. H. 8-plex quantitation of changes in cerebrospinal fluid protein expression in subjects undergoing intravenous immunoglobulin treatment for Alzheimer's disease. *Proteomics* **2007**, *7* (20), 3651−3660.

(6) Dayon, L.; Hainard, A.; Licker, V.; Turck, N.; Kuhn, K.; Hochstrasser, D. F.; Burkhard, P. R.; Sanchez, J. C. Relative quantification of proteins in human cerebrospinal fluids by MS/MS using 6-plex isobaric tags. *Anal. Chem.* **2008**, *80* (8), 2921−2931.

(7) Gevaert, K.; Impens, F.; Ghesquiere, B.; Van Damme, P.; Lambrechts, A.; Vandekerckhove, J. Stable isotopic labeling in proteomics. *Proteomics* **2008**, *8* (23−24), 4873−4885.

(8) Boersema, P. J.; Aye, T. T.; van Veen, T. A. B.; Heck, A. J. R.; Mohammed, S. Triplex protein quantification based on stable isotope labeling by peptide dimethylation applied to cell and tissue lysates. *Proteomics* **2008**, *8* (22), 4624−4632.

(9) Kim, J. S.; Fillmore, T. L.; Liu, T.; Robinson, E.; Hossain, M.; Champion, B. L.; Moore, R. J.; Camp, D. G.; Smith, I. R. D.; Qian, W. J. O-18-Labeled Proteome Reference as Global Internal Standards for Targeted Quantification by Selected Reaction Monitoring-Mass Spectrometry. *Mol. Cell. Proteomics* **2011**, *10* (12), M110.007302.

(10) Rauniyar, N.; Yates, J. R., 3rd Isobaric labeling-based relative quantification in shotgun proteomics. *J. Proteome Res.* **2014**, *13* (12), 5293−5309.

(11) Larance, M.; Lamond, A. I. Multidimensional proteomics for cell biology. *Nat. Rev. Mol. Cell Biol.* **2015**, *16* (5), 269−280.

(12) Ow, S. Y.; Salim, M.; Noirel, J.; Evans, C.; Rehman, I.; Wright, P. C. iTRAQ underestimation in simple and complex mixtures: "the good, the bad and the ugly". *J. Proteome Res.* **2009**, *8* (11), 5347−5355.

(13) Karp, N. A.; Huber, W.; Sadowski, P. G.; Charles, P. D.; Hester, S. V.; Lilley, K. S. Addressing accuracy and precision issues in iTRAQ quantitation. *Mol. Cell. Proteomics* **2010**, *9* (9), 1885−97.

(14) Ting, L.; Rad, R.; Gygi, S. P.; Haas, W. MS3 eliminates ratio distortion in isobaric multiplexed quantitative proteomics. *Nat. Methods* **2011**, *8* (11), 937−940.

(15) McAlister, G. C.; Nusinow, D. P.; Jedrychowski, M. P.; Wuhr, M.; Huttlin, E. L.; Erickson, B. K.; Rad, R.; Haas, W.; Gygi, S. P. MultiNotch MS3 enables accurate, sensitive, and multiplexed detection of differential expression across cancer cell line proteomes. *Anal. Chem.* **2014**, *86* (14), 7150−8.

(16) Erickson, B. K.; Rose, C. M.; Braun, C. R.; Erickson, A. R.; Knott, J.; McAlister, G. C.; Wuhr, M.; Paulo, J. A.; Everley, R. A.; Gygi, S. P. A Strategy to Combine Sample Multiplexing with Targeted Proteomics Assays for High-Throughput Protein Signature Characterization. *Mol. Cell* **2017**, *65* (2), 361−370.

(17) Mertins, P.; Udeshi, N. D.; Clauser, K. R.; Mani, D. R.; Patel, J.; Ong, S. E.; Jaffe, J. D.; Carr, S. A. iTRAQ labeling is superior to mTRAQ for quantitative global proteomics and phosphoproteomics. *Mol. Cell. Proteomics* **2012**, *11* (6), M111.014423.

(18) Chen, X.; Wei, S.; Ji, Y.; Guo, X.; Yang, F. Quantitative proteomics using SILAC: Principles, applications, and developments. *Proteomics* **2015**, *15* (18), 3175−3192.

(19) Boersema, P. J.; Raijmakers, R.; Lemeer, S.; Mohammed, S.; Heck, A. J. Multiplex peptide stable isotope dimethyl labeling for quantitative proteomics. *Nat. Protoc.* **2009**, *4* (4), 484−494.

(20) Kleifeld, O.; Doucet, A.; auf dem Keller, U.; Prudova, A.; Schilling, O.; Kainthan, R. K.; Starr, A. E.; Foster, L. J.; Kizhakkedathu, J. N.; Overall, C. M. Isotopic labeling of terminal amines in complex samples identifies protein N-termini and protease cleavage products. *Nat. Biotechnol.* **2010**, *28* (3), 281−288.

(21) Schilling, O.; Barre, O.; Huesgen, P. F.; Overall, C. M. Proteome-wide analysis of protein carboxy termini: C terminomics. *Nat. Methods* **2010**, *7* (7), 508−511.

(22) Schilling, O.; Huesgen, P. F.; Barre, O.; auf dem Keller, U.; Overall, C. M. Characterization of the prime and non-prime active site specificities of proteases by proteome-derived peptide libraries and tandem mass spectrometry. *Nat. Protoc.* **2011**, *6* (1), 111−120.

(23) Hettinger, J.; Richards, D. M.; Hansson, J.; Barra, M. M.; Joschko, A. C.; Krijgsveld, J.; Feuerer, M. Origin of monocytes and macrophages in a committed progenitor. *Nat. Immunol.* **2013**, *14* (8), 821−830.

(24) Shan, B.; Xu, C. P.; Zhang, Y. Y.; Xu, T.; Gottesfeld, J. M.; Yates, J. R. Quantitative Proteomic Analysis Identifies Targets and Pathways of a 2-Aminobenzamide HDAC Inhibitor in Friedreich's Ataxia Patient iPSC-Derived Neural Stem Cells. *J. Proteome Res.* **2014**, *13* (11), 4558−4566.

(25) Babin, B. M.; Bergkessel, M.; Sweredoski, M. J.; Moradian, A.; Hess, S.; Newman, D. K.; Tirrell, D. A. SutA is a bacterial transcription factor expressed during slow growth in Pseudomonas aeruginosa. *Proc. Natl. Acad. Sci. U. S. A.* **2016**, *113* (5), E597−605.

DOI: 10.1021/acs.jproteome.8b00775
J. Proteome Res. 2019, 18, 1078−1087

(26) Choi, J.; Xu, M.; Makowski, M. M.; Zhang, T.; Law, M. H.; Kovacs, M. A.; Granzhan, A.; Kim, W. J.; Parikh, H.; Gartside, M.; Trent, J. M.; Teulade-Fichou, M. P.; Iles, M. M.; Newton-Bishop, J. A.; Bishop, D. T.; MacGregor, S.; Hayward, N. K.; Vermeulen, M.; Brown, K. M. A common intronic variant of PARP1 confers melanoma risk and mediates melanocyte growth via regulation of MITF. *Nat. Genet.* **2017**, *49* (9), 1326−1335.
(27) Zhang, R.; Sioma, C. S.; Thompson, R. A.; Xiong, L.; Regnier, F. E. Controlling deuterium isotope effects in comparative proteomics. *Anal. Chem.* **2002**, *74* (15), 3662−3669.
(28) Valleix, A.; Carrat, S.; Caussignac, C.; Leonce, E.; Tchapla, A. Secondary isotope effects in liquid chromatography behaviour of 2H and 3H labelled solutes and solvents. *Journal of chromatography A* **2006**, *1116* (1−2), 109−126.
(29) Lau, H. T.; Suh, H. W.; Golkowski, M.; Ong, S. E. Comparing SILAC- and stable isotope dimethyl-labeling approaches for quantitative proteomics. *J. Proteome Res.* **2014**, *13* (9), 4164−4174.
(30) Barrios-Llerena, M. E.; Pritchard, J. C.; Kerr, L. E.; Le Bihan, T. The use of a novel quantitation strategy based on Reductive Isotopic Di-Ethylation (RIDE) to evaluate the effect of glufosinate on the unicellular algae Ostreococcus tauri. *J. Proteomics* **2011**, *74* (12), 2798−2809.
(31) Mortera, S. L.; Dioni, I.; Greco, V.; Neri, C.; Rovero, P.; Urbani, A. pH-regulated formation of side products in the reductive amination approach for differential labeling of peptides in relative quantitative experiments. *Electrophoresis* **2014**, *35* (9), 1259−1267.
(32) Koehler, C. J.; Arntzen, M. O.; Thiede, B. The impact of carbon-13 and deuterium on relative quantification of proteins using stable isotope diethyl labeling. *Rapid Commun. Mass Spectrom.* **2015**, *29* (9), 830−836.
(33) Kim, H.; Vick, P.; Hedtke, J.; Ploper, D.; De Robertis, E. M. Wnt Signaling Translocates Lys48-Linked Polyubiquitinated Proteins to the Lysosomal Pathway. *Cell Rep.* **2015**, *11* (8), 1151−1159.
(34) Peuchen, E. H.; Sun, L.; Dovichi, N. J. Optimization and comparison of bottom-up proteomic sample preparation for early-stage Xenopus laevis embryos. *Anal. Bioanal. Chem.* **2016**, *408* (17), 4743−4749.
(35) Wilson-Grady, J. T.; Haas, W.; Gygi, S. P. Quantitative comparison of the fasted and re-fed mouse liver phosphoproteomes using lower pH reductive dimethylation. *Methods* **2013**, *61* (3), 277−286.
(36) Cox, J.; Mann, M. MaxQuant enables high peptide identification rates, individualized p.p.b.-range mass accuracies and proteome-wide protein quantification. *Nat. Biotechnol.* **2008**, *26* (12), 1367−1372.
(37) Wuhr, M.; Freeman, R. M., Jr.; Presler, M.; Horb, M. E.; Peshkin, L.; Gygi, S.; Kirschner, M. W. Deep proteomics of the Xenopus laevis egg using an mRNA-derived reference database. *Curr. Biol.* **2014**, *24* (13), 1467−1475.
(38) Fu, Q.; Li, L. De novo sequencing of neuropeptides using reductive isotopic methylation and investigation of ESI QTOF MS/MS fragmentation pattern of neuropeptides with N-terminal dimethylation. *Anal. Chem.* **2005**, *77* (23), 7783−7795.
(39) Ji, C.; Lo, A.; Marcus, S.; Li, L. Effect of 2MEGA labeling on membrane proteome analysis using LC-ESI QTOF MS. *J. Proteome Res.* **2006**, *5* (10), 2567−2576.
(40) Brauman, J. I.; Riveros, J. M.; Blair, L. K. Gas-Phase Basicities of Amines. *J. Am. Chem. Soc.* **1971**, *93* (16), 3914−3916.
(41) Petritis, K.; Kangas, L. J.; Yan, B.; Monroe, M. E.; Strittmatter, E. F.; Qian, W. J.; Adkins, J. N.; Moore, R. J.; Xu, Y.; Lipton, M. S.; Camp, D. G., 2nd; Smith, R. D. Improved peptide elution time prediction for reversed-phase liquid chromatography-MS by incorporating peptide sequence information. *Anal. Chem.* **2006**, *78* (14), 5026−5039.
(42) Ji, C. J.; Li, W. L.; Ren, X. D.; El-Kattan, A. F.; Kozak, R.; Fountain, S.; Lepsy, C. Diethylation Labeling Combined with UPLC/MS/MS for Simultaneous Determination of a Panel of Monoamine Neurotransmitters in Rat Prefrontal Cortex Microdialysates. *Anal. Chem.* **2008**, *80* (23), 9195−9203.
(43) Shi, T.; Fillmore, T. L.; Sun, X.; Zhao, R.; Schepmoes, A. A.; Hossain, M.; Xie, F.; Wu, S.; Kim, J. S.; Jones, N.; Moore, R. J.; Pasa-Tolic, L.; Kagan, J.; Rodland, K. D.; Liu, T.; Tang, K.; Camp, D. G., 2nd; Smith, R. D.; Qian, W. J. Antibody-free, targeted mass-spectrometric approach for quantification of proteins at low picogram per milliliter levels in human plasma/serum. *Proc. Natl. Acad. Sci. U. S. A.* **2012**, *109* (38), 15395−15400.
(44) Wang, Y.; Yang, F.; Gritsenko, M. A.; Wang, Y.; Clauss, T.; Liu, T.; Shen, Y.; Monroe, M. E.; Lopez-Ferrer, D.; Reno, T.; Moore, R. J.; Klemke, R. L.; Camp, D. G., 2nd; Smith, R. D. Reversed-phase chromatography with multiple fraction concatenation strategy for proteome profiling of human MCF10A cells. *Proteomics* **2011**, *11* (10), 2019−2026.
(45) Tolonen, A. C.; Haas, W. Quantitative proteomics using reductive dimethylation for stable isotope labeling. *J. Visualized Exp.* **2014**, *89*, No. e51416.
(46) Yu, C. L.; Brooks, S.; Li, Y.; Subramanian, M.; Summers, R.; Pope, M. Rapid Proteomics to Prospect and Validate Novel Bacterial Metabolism Induced by Environmental Burden. *Methods Enzymol.* **2017**, *586*, 379−411.
(47) Wuhr, M.; Haas, W.; McAlister, G. C.; Peshkin, L.; Rad, R.; Kirschner, M. W.; Gygi, S. P. Accurate multiplexed proteomics at the MS2 level using the complement reporter ion cluster. *Anal. Chem.* **2012**, *84* (21), 9214−9221.
(48) Peshkin, L.; Wuhr, M.; Pearl, E.; Haas, W.; Freeman, R. M., Jr.; Gerhart, J. C.; Klein, A. M.; Horb, M.; Gygi, S. P.; Kirschner, M. W. On the Relationship of Protein and mRNA Dynamics in Vertebrate Embryonic Development. *Dev. Cell* **2015**, *35* (3), 383−394.
(49) Sun, L.; Bertke, M. M.; Champion, M. M.; Zhu, G.; Huber, P. W.; Dovichi, N. J. Quantitative proteomics of Xenopus laevis embryos: expression kinetics of nearly 4000 proteins during early development. *Sci. Rep.* **2015**, *4*, 4365.
(50) Wyant, G. A.; Abu-Remaileh, M.; Frenkel, E. M.; Laqtom, N. N.; Dharamdasani, V.; Lewis, C. A.; Chan, S. H.; Heinze, I.; Ori, A.; Sabatini, D. M. NUFIP1 is a ribosome receptor for starvation-induced ribophagy. *Science* **2018**, *360* (6390), 751−758.
(51) Guo, K.; Ji, C. J.; Li, L. Stable-isotope dimethylation labeling combined with LC-ESI MS for quantification of amine-containing metabolites in biological samples. *Anal. Chem.* **2007**, *79* (22), 8631−8638.

DOI: 10.1021/acs.jproteome.8b00775
J. Proteome Res. 2019, 18, 1078−1087